

Discovery of a new, 2.2 Mpc Giant Radio Galaxy at a redshift of 0.57

Biny Sebastian¹, C.H. Ishwara-Chandra¹, Ravi Joshi^{2,3}, Yogesh Wadadekar^{1,*}

¹National Centre for Radio Astrophysics, TIFR, Post Bag No. 3, Ganeshkhind Post, Pune, India

²Inter University Centre for Astronomy and Astrophysics, Post Bag No. 4, Ganeshkhind Post, Pune, India

³Kavli Institute for Astronomy and Astrophysics, Peking University, Beijing 100871, China

Accepted XXX. Received YYY; in original form ZZZ

ABSTRACT

We report the discovery of one of the largest and most distant Giant Radio Galaxy (GRG) in the Lynx field which was discovered using deep Giant Metre-wave Radio Telescope (GMRT) 150 MHz observations. The core is detected at 150 MHz and also in the VLA FIRST survey. Spectroscopic observations carried out using the IUCAA Girawali Observatory (IGO) provided a redshift value of 0.57. This redshift was later confirmed with data from the Sloan Digital Sky Survey (Data Release 12). The angular size of the GRG is 5.5 arcmin and at the redshift of 0.57, its linear size is 2.2 Mpc. At this high redshift, only a few radio sources are known to have such large linear size. In order to estimate the spectral index of the bridge emission as well as the spectral age of the source, we observed this source at L-band, 610 MHz and 325 MHz bands with the GMRT. We present the spectral ageing analysis of the source which puts an upper limit of 20 Myr on the spectral age. The better resolution maps presented here as opposed to the original 150 MHz map shows evidence for a second episode of emission. We also find that the core is detected at all four frequencies with a spectral index of 0.85, which is steeper than normal, hence we speculate that the core may be a compact steep spectrum source (CSS), which makes this giant radio galaxy a candidate triple-double radio galaxy.

Key words: galaxies: active - galaxies: high-redshift - radio continuum: galaxies

1 INTRODUCTION

A small fraction of active galaxies (AGNs) exhibits powerful radio emission on either side of the nuclei of the galaxies. The majority of such radio sources are compact in size. However, a tiny fraction of them do attain sizes over a mega parsec and are known as 'Giant Radio Sources' (GRS). Their large linear size (> 1 Mpc) makes them interesting candidates to understand the evolution of radio sources and to study the ambient intergalactic medium which confines the lobes so far away from the parent galaxy. However, detecting such giant radio sources becomes difficult because the bridge emission connecting the two lobes is often not seen. Low-frequency radio surveys are better suited to search for this population (Schoenmakers et al. 2000) as compared to higher frequency radio surveys because the aged plasma will have a steep spectrum and is brighter at low frequencies.

Till date, more than 300 giant radio galaxies have been discovered (Dabhade et al. (2017); Ishwara-Chandra

& Saikia (1999); Schoenmakers et al. (2001); Lara et al. (2001), Subrahmanyam et al. (1996); Machalski et al. (2001), Machalski et al. (2006), Saripalli et al. (2005), Solov'yov & Verkhodanov (2014)), Tamhane et al. (2015)). The longest identified giant radio galaxy is J1420-0545 with a linear size of 4.69 Mpc (Machalski et al. (2008)). Proctor (2016) classified 1700 radio sources from the NVSS catalog as giant radio sources based on their angular extent using a pattern recognition algorithm. Because large angular extents are used as primary criteria while classifying giant radio galaxies, the number of giant radio sources identified at high redshifts is low. Most of them are nearby ($z \lesssim 0.5$) and with a linear size smaller than 2 Mpc. Increasing the number of identified giant radio galaxies at high redshift is necessary for studying the evolution of the radio galaxy population over redshift.

Numerous studies were undertaken to understand the reason for the large linear sizes of these sources. The dynamical age of these sources suggest these have evolved over long periods of time (Kaiser & Alexander 1997). However, Mack et al. (1998) find spectral ages comparable to the radio galaxies with normal sizes. Hence, they conclude the large

* E-mail: biny@ncra.tifr.res.in (BS)

linear sizes are probably due to the low density of the intergalactic medium surrounding the giant radio sources. Many authors have also investigated the role of the nuclear host power in creating these giant sources. [Ishwara-Chandra & Saikia \(1999\)](#) find that the giant radio galaxies have similar core strengths compared to the rest of the radio galaxies of normal sizes having comparable luminosity. It is also interesting to note that several of the giant radio sources show recurrent jet activity ([Konar & Hardcastle \(2013\)](#), [Kronberg et al, 2001](#)). Though the mechanism which leads to the stopping and restarting of radio galaxies is still not well understood, there are models which invoke galaxy mergers to explain the episodic jet activity. For example, [Liu et al. \(2003\)](#) suggests that the disruption of the accretion disk due to the inspiral of a second SMBH into the larger one causes an interruption in the jet activity.

The spectral ageing analysis is an invaluable tool in tracing the evolution of radio galaxies. Due to the large angular extent of giant radio galaxies, we can learn more about various energy loss and gain mechanisms of the radiating particles at different locations individually like the hotspots, lobes, etc. It was noted previously by [Ishwara-Chandra & Saikia \(1999\)](#) and [Schoenmakers et al. 2000a](#) that inverse Compton losses dominate the synchrotron losses in the lobes of giant radio galaxies. Moreover, galaxies at higher redshifts are expected to have higher inverse Compton losses due to denser cosmic microwave background. Also understanding spectral index variations across the lobes in a normal population of radio sources at higher redshifts is hard because of their low angular widths. Hence giant radio galaxies at higher redshifts help us get a better handle on the spectral ageing and evolution studies at higher redshifts.

In this paper, we report the discovery of a giant radio source of linear size 2.2 Mpc at 0.57 redshift in the LBDS-Lynx field. The paper is organised as follows. The details of observations and data analysis techniques used are elaborated in Section 2. Section 3 discusses several results derived from morphological and spectral ageing analysis.

We used a cosmology, with $\Omega_M = 0.286$, $\Omega_{baryon} = 0.0463$ and $H_0 = 69.3 \text{ km s}^{-1} \text{ Mpc}^{-1}$.

2 OBSERVATIONS AND DATA ANALYSIS

The LBDS(Leiden Berkeley Deep Survey)-Lynx field was observed with Giant-Metrowave Radio Telescope (GMRT) at 150 MHz to search for high-redshift radio galaxies ([Ishwara-Chandra et al. 2010](#)). A candidate giant radio source was found in the field, beyond the half-power beam width with an RA DEC of 08h44m08.8s +46d27m44s.

The core was also detected in the VLA FIRST survey data. An SDSS counterpart was identified with a red galaxy having a photometric redshift of 0.62 and R band magnitude of 21.9 ([Abazajian et al. 2009](#)). The angular size of the radio source was $5.5'$ and at a redshift of 0.62, the linear size of the galaxy is ~ 2.3 Mpc. In the 150 MHz image, the radio lobes were barely seen. To further characterize the giant radio galaxy, deep radio observations with GMRT and spectroscopic observations with IUCAA Girawali 2.0 m optical telescope were carried out. The details of the radio and optical observations are given below.

2.1 GMRT observations and data analysis

GMRT observations were carried out at three frequencies, 325 MHz (P-band), 610 MHz, 1250 MHz (L-band). The details of the GMRT observations used for imaging are given in Table 1. The observations at 610 MHz and 325 MHz were carried out using the legacy system. The observation in L-band was done using the new upgraded GMRT (uGMRT) with a wideband backend mostly using central square antennas to detect the bridge emission. The basic editing was carried out using the Astronomical Imaging Processing Software (AIPS). Bad data were identified and flagged, and calibration was carried out using standard tasks. Radio Frequency Interference (RFI) was identified and flagged after bandpass calibration. The bandpass calibration was rerun after the flagging of RFI. The target file was SPLIT after final calibration. For data sets at 325 MHz and 610 MHz, images were made in AIPS using standard procedures. Several rounds of phase-only self-calibration were done to remove phase errors due to the ionosphere. Since the L-band data had a bandwidth of 400 MHz, it was not possible to image in AIPS due to the unavailability of the MS-MFS (Multi-Scale-Multi Frequency Synthesis) algorithm. So the imaging was done in CASA using the task 'clean.' There were two data sets in L-band, which were combined in UV plane using the task CONCAT. The wide band data were also divided into 8 split files of 50 MHz bandwidth each. Each split file was then imaged and self-calibrated individually after which all of them were combined back in UV-plane in CASA for final imaging. As a final step, primary beam correction was done for all the images. The angular size of the source was ~ 5 arcmin which is well within the HPBW (28 arcmins), therefore single primary beam correction at L-band at the central frequency of the band is justified.

For the spectral ageing analysis, images were made with matching uvranges at different frequencies. Uniform weighting was used while making these images. This procedure is adopted to make sure that the amount of diffuse emission picked up at different frequencies is similar. The relative shift between the two maps was corrected for and was then convolved to the same beam before making the spectral index maps. Spectral index maps were made from 610 and 325 MHz maps using task COMB in AIPS.

2.2 Optical Spectroscopic Observations

Spectroscopic observations were carried out using the 2 m optical telescope at the IUCAA Girawali Observatory (IGO) to find out the spectroscopic redshift. O[II] and O[III] lines are clearly detected. The spectrum is shown in Figure 1. The spectroscopic redshift was estimated to be 0.5692 ± 0.0001 . Subsequently, independent spectroscopic observations from the SDSS DR12 data release ([Alam et al. 2015](#)) of the corresponding object, SDSS J084408.85+462744.2 confirmed the redshift

3 RESULTS

Here we present the results of radio observations and spectral ageing analysis. The core and bridge emission is clearly

Table 1. GMRT Observation Details

Central Frequency (MHz)	Flux Calibrator	Phase Calibrator	Bandwidth	Time on source	Number of antennas	Observation Date
325	3C147	0834+555	32MHz	3.7h	27	15-Sep-2009
610	3C147, 3C286	0834+555	32 MHz	8h	29	06-May-2010
	3C147, 3C286	0834+555	32 MHz	3h	29	29-Nov-2015
1250	3C147	0834+555	400MHz	2.5h	16	01-Sep-2015
	3C147,3C286	0834+555	400MHz	5h	16 (11/16 Central Square)	07-Nov-2015
					16 (14/16 Central Square)	

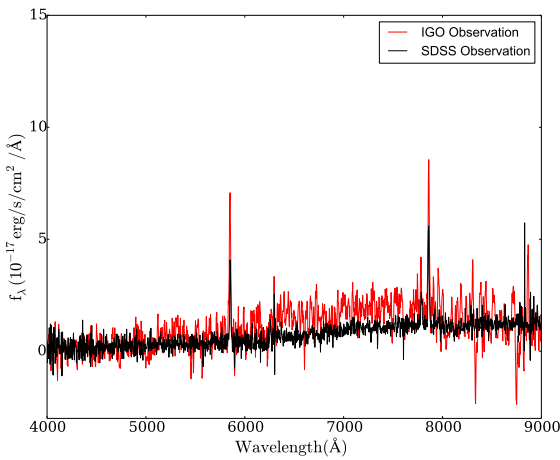


Figure 1. Optical Spectrum of J084408+462744: The spectrum in red was obtained using observations from the 2-m telescope at IUCAA Girawali Observatory. IGO spectrum is not flux calibrated. The spectrum in black was obtained from SDSS.

detected at 325, 610 and 1400 MHz. The core is unresolved in all the three bands. The details are as below.

3.1 Morphology

The contour maps at 4σ level for all the three frequencies are shown in Figure 3. The giant radio galaxy has a linear morphology with no noticeable distortions. Saripalli & Subrahmanyam (2009) points out that giant radio galaxies, in general, are free from any winged emission or distortions in the bridges. They also show that the jet axis of giant radio galaxy population is commonly aligned along the optical minor axis. Hence, the absence of distortions suggests that the large sizes of this giant galaxy might also be due to the ejection in a direction of least resistance or the steepest pressure gradient. The core is bright indicating the presence of ongoing activity. The hotspots, core and the lobes are clearly detected in all three frequency maps. The jet is not detected. A closer look at the lobes towards south shows tightening of contours almost halfway between the core and the final hotspot. A similar brightening in flux density is found midway on the other side as well. If this tightening is arising from yet another pair of hotspot, then this giant radio galaxy might be a double-double radio galaxy. The inner

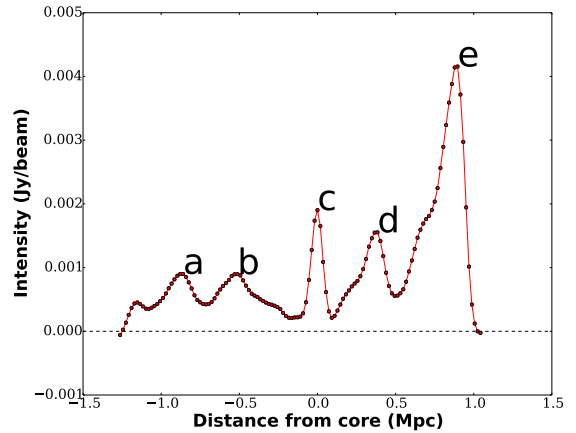


Figure 2. The spatial profile of intensity along the length of the giant radio galaxy

pair of lobes is well aligned with the outer ones. However, in most double-double radio galaxies, the inner hotspot is narrower compared to the outer one owing to the clearing of the path due to the previous ejection. The variation of intensity along the ridgeline of the giant radio galaxy at 610 MHz is plotted as a function of distance from the core in Figure 2. This plot clearly shows the asymmetry of the giant radio source. The point c marks the location of the core. Points a and e correspond to seemingly the first epoch of radio emission. However, there is no hotspot towards the north and also the emission fades away after the peak of brightness. There is a difference of 0.2 Mpc in the total lengths of the lobes from the core to both the sides as is seen in Figure 2. The brightness peaks corresponding to the 2nd epoch are also displaced by 0.1 Mpc distance. This difference might be arising due to the difference in the environments in which they reside. This might indicate that the hotspot advance speed is much lower towards the south due to a denser environment. The radio power near the FR-I/FR-II divide and also the absence of hotspots towards the northern side makes the classification of this object as FR-II questionable. This absence could also be an after effect of a disruption in continuous energy supply from the central engine combined with a low-density environment.

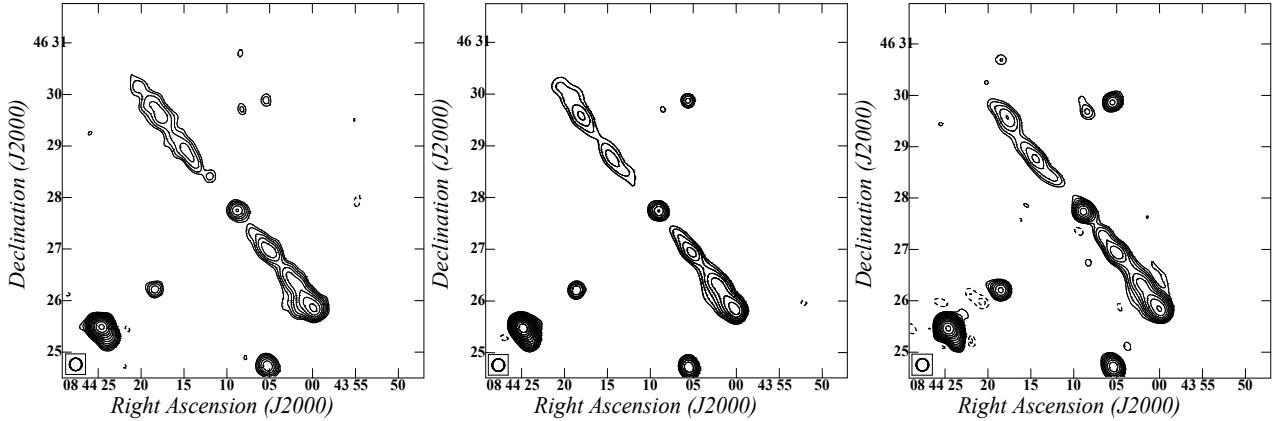


Figure 3. Left-hand panel: Image at 325 MHz, peak surface brightness is $57.2 \text{ mJy beam}^{-1}$, the rms is $0.2 \text{ mJy beam}^{-1}$ Middle panel: Image at 610 MHz, the peak surface brightness is $25.5 \text{ mJy beam}^{-1}$, the rms is $0.1 \text{ mJy beam}^{-1}$ Right hand panel: Image at 1250 MHz, the peak surface brightness is $12.4 \text{ mJy beam}^{-1}$, the rms is $0.03 \text{ mJy beam}^{-1}$. Contour levels of all maps are $4\sigma \times (-2, -1.40, -1, 1, 1.400, 2, 2.800, 4, 5.600, 8, 11.20, 16, 23)$. All maps have been convolved to a beam size of $14''.5 \times 14''.5$

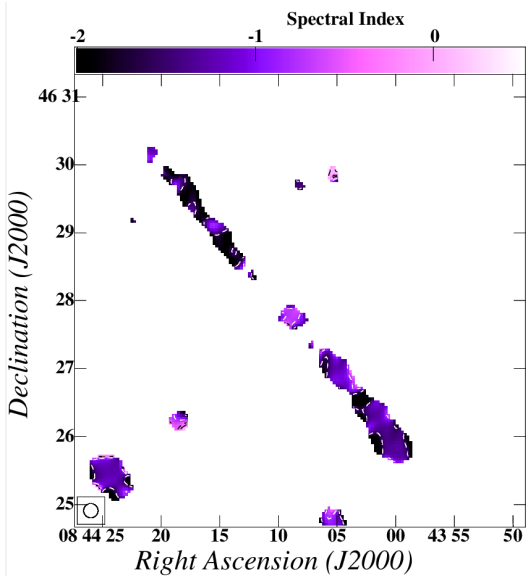


Figure 4. 325-610 MHz Spectral index map of the giant radio galaxy.

3.2 Spectral Ageing Analysis

The higher energy electrons from a synchrotron radiation emitting population lose their energy faster compared to the low energy ones. As a result, there is a steepening of the energy distribution of the electron population which in turn leads to steepening of the spectrum over time, and the depletion of the high-energy electrons also introduces a break in the radio spectrum. The break frequency shifts to lower frequencies over time. The age of the synchrotron plasma can be estimated by using the value of the spectral index and also the value of the break in the spectrum. Hotspots are thought to provide in-situ acceleration, and it is assumed that the electrons are not accelerated anymore after it leaves the hotspot. Hence in typical FR-II radio galaxies, the spec-

trum is flatter at hotspots and it then steepens in the lobe towards the core.

Figure 4 shows the spectral index map made using images at 325 and 610 MHz. At the position of the hotspot which is suspected to have formed as a result of the second epoch of injection, the spectrum is flatter compared to the regions beyond it. This flattening in spectra is also seen towards the northern lobe as well. The increase in luminosity at these positions as was elaborated in the previous section coupled with the flattening of the spectrum makes it extremely likely that it is indeed a double-double radio galaxy. It is hard to explain the abrupt increase in net energy of electrons in the backflow, without invoking injection of a fresh population of electrons.

The spectral ageing analysis could act as a powerful tool to probe whether the object is indeed a double-double radio galaxy. The new hotspot would be expected to contain a younger population of electrons due to fresh injection. The difference in spectral age would also give a rough idea about timescales of episodic emission in such galaxies.

Spectral age is defined as the time which has elapsed since the electrons were last accelerated. Hence, the hotspots are expected to have the least spectral age. The net radiative losses from the hotspots and lobes are attributed to synchrotron and inverse-Compton loss mechanism. The adiabatic losses are neglected. Though it doesn't change the steepening of the spectrum, it shifts the break frequency to lower values. This may lead to the over estimation of the spectral age.

$$\tau_{spec} = \frac{B^{1/2}}{B^2 + B_{ic}^2} (\nu_{br}(1+z))^{-1/2} \quad (1)$$

where $B_{ic} = 0.318(1+z)^2$ is the equivalent magnetic field of cosmic microwave background radiation at redshift z , B is the magnetic field strength of the lobes, ν_{br} is the break frequency in GHz. Both magnetic fields are expressed in units of nT (Jamrozny et al. 2008).

As is clear from the equation, one needs to know the magnetic field at different locations and also the break frequencies to estimate the age. Equipartition magnetic field

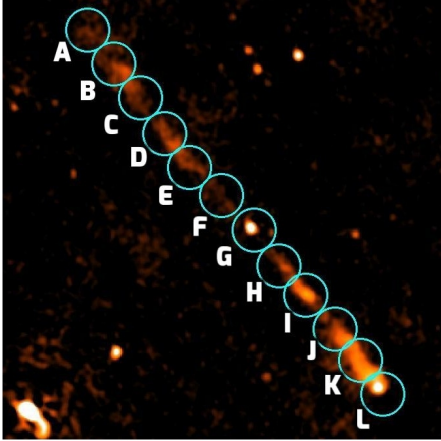


Figure 5. Different regions taken to calculate spectral age

Table 2. Values of Equipartition Magnetic field estimated at different regions

Region	Magnetic Field(μG)
A	1.07 ± 0.22
B	1.08 ± 0.21
C	1.00 ± 0.29
D	1.24 ± 0.22
E	0.80 ± 0.10
F	0.57 ± 0.13
H	0.74 ± 0.08
I	1.02 ± 0.04
J	0.99 ± 0.09
K	1.30 ± 0.20
L	1.16 ± 0.15

was used as a proxy for the physical magnetic field assuming minimum energy conditions (Moffet 1975).

$$B_{eq} = 2.3(aAL/V)^{2/7} \quad (2)$$

Since the giant radio galaxy covers a significant number of resolution elements, spectral ageing analysis can be done for different regions separately. The giant radio galaxy was split into 12 circular regions as shown in Figure 5. The flux values were noted for each region separately except for region G which marks the position of the core, and the spectral index value for each region was calculated by fitting a power law. Interestingly none of the regions showed any curvature or deviation from power law at higher frequencies (i.e., L-band), which means the break is at much higher frequencies. The spectral index values, luminosities and volume of each region was used to calculate the equipartition magnetic field at all the regions. Cylindrical symmetry was assumed while calculating the magnetic field. The ratio of a number of electrons to protons was chosen to be 1. The magnetic field at different regions is listed out in the Table 2 except for region G which marks the position of the core.

Table 3. Values of the flux density of the core at different frequencies

Frequency(MHz)	Core Flux density(mJy)	Error
150	9.2	± 4.2
325	4.8	± 0.3
610	2.5	± 0.4
1250	1.5	± 1.0

The spectra followed a power law from 325 MHz to 1.4 GHz and since there was no evidence for any break up to 1.4 GHz, we didn't fit the spectrum with standard models like the JaffePerola (JP; Jaffe & Perola (1973)) and the KardashevPacholczyk (KP; Kardashev (1962); Pacholczyk (1970)) models. Instead, 1.4 GHz was chosen as the lower limit on the break frequency, which puts an upper limit on the spectral ages.

This upper limit was calculated using the equation (1).

The upper limit on ages ranges from 13 Myr – 20 Myr. Jamroz et al. (2008) finds spectral ages in the range of 6 to 36 Myr and a median spectral age of 22 Myr for a sample of eight giant radio galaxies. Though an upper limit, the spectral age of the giant radio galaxy suggests that it fits in with the general population of giant radio galaxies.

3.3 Core Spectrum

The core is unresolved in all the four frequencies from 150 MHz to 1.4 GHz. The core spectrum is unusually steep ($\alpha = -0.85$) for a compact object. There is no turnover even at 150 MHz. In general, for a compact core of AGN, one would expect it to have a flatter spectrum and show turnover or evidence of turnover at lower frequencies due to synchrotron self absorption. The highest resolution image corresponds to 3 arcsec. This angular width corresponds to about 20 kpc. This suggests the presence of yet another pair of lobes near the core. High frequency observations with sub-arcsec resolution could resolve another pair of lobe if any. The core spectrum is shown in Figure 6 and the core flux densities are listed in Table 3.

4 DISCUSSION AND CONCLUSIONS

We have discovered a giant radio galaxy in the field of Lynx. The giant radio galaxy was detected at all the three observed frequencies including 325, 610 and 1250 MHz. The redshift was estimated using optical observations taken by IUCAA Girawali Observatory and was later confirmed with SDSS DR12 data release. The angular size of 5.5 arcmin translates to a linear size of 2.2 Mpc at the redshift 0.57. The total flux density of the giant radio source at 325 MHz is 82.3 mJy which corresponds to a specific luminosity of $1.07 \times 10^{33} \text{ ergs s}^{-1} \text{ Hz}^{-1}$. This giant radio source is linear in structure and shows no evidence for distortions in the bridges. The contour maps show evidence for edge brightening in the lobe towards the south, while the hot spot is

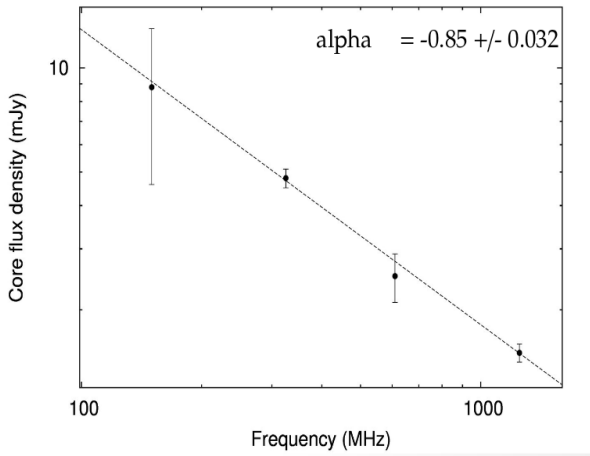


Figure 6. Spectrum of the core

not very clearly identifiable in the northern lobe. This edge brightening almost halfway the full length of the giant radio galaxy might be due to a difference in environments. The IGM might be relatively less dense to the northern side. Given that the lobes are separated by distances as large as 2 Mpc, it is possible that the environments are considerably different. The equipartition magnetic field in the lobes of the giant radio galaxy was estimated to have an average value of $1.00\mu\text{G}$. Using the estimated equipartition magnetic field at different regions and a lower limit on the break frequency at 1400 MHz, an upper limit of spectral age was estimated as 20 Myr. The giant radio galaxy shows some evidence for episodic emission. The steep-spectrum of the core also suggests the presence of yet another pair of lobes unresolved within the core and this giant radio galaxy turns out to be a candidate triple-double radio galaxy.

ACKNOWLEDGEMENTS

We thank the anonymous referee for her or his comments and suggestions which helped in improving the manuscript. We thank the staff of the GMRT that made these observations possible. GMRT is run by the National Centre for Radio Astrophysics of the Tata Institute of Fundamental Research. We wish to acknowledge the IUCAA/IGO staff for their support during our observations.

Funding for the Sloan Digital Sky Survey IV has been provided by the Alfred P. Sloan Foundation, the U.S. Department of Energy Office of Science, and the Participating Institutions. SDSS-IV acknowledges support and resources from the Center for High-Performance Computing at the University of Utah. The SDSS web site is www.sdss.org.

SDSS-IV is managed by the Astrophysical Research Consortium for the Participating Institutions of the SDSS Collaboration including the Brazilian Participation Group, the Carnegie Institution for Science, Carnegie Mellon University, the Chilean Participation Group, the French Participation Group, Harvard-Smithsonian Center for Astrophysics, Instituto de Astrofísica de Canarias, The Johns Hopkins University, Kavli Institute for the Physics and

Mathematics of the Universe (IPMU) / University of Tokyo, Lawrence Berkeley National Laboratory, Leibniz Institut für Astrophysik Potsdam (AIP), Max-Planck-Institut für Astronomie (MPIA Heidelberg), Max-Planck-Institut für Astrophysik (MPA Garching), Max-Planck-Institut für Extraterrestrische Physik (MPE), National Astronomical Observatories of China, New Mexico State University, New York University, University of Notre Dame, Observatório Nacional / MCTI, The Ohio State University, Pennsylvania State University, Shanghai Astronomical Observatory, United Kingdom Participation Group, Universidad Nacional Autónoma de México, University of Arizona, University of Colorado Boulder, University of Oxford, University of Portsmouth, University of Utah, University of Virginia, University of Washington, University of Wisconsin, Vanderbilt University, and Yale University.

REFERENCES

- Abazajian, K. N., Adelman-McCarthy, J. K., Agüeros, M. A., et al. 2009, *ApJS*, 182, 543-558
- Alam, S., Albareti, F. D., Allende Prieto, C., et al. 2015, *ApJS*, 219, 12
- Dabhade, P., Gaikwad, M., Bagchi, J., et al. 2017, arXiv:1704.00516
- Ishwara-Chandra, C. H., & Saikia, D. J. 1999, *MNRAS*, 309, 100
- Ishwara-Chandra, C. H., Sirothia, S. K., Wadadekar, Y., Pal, S., & Windhorst, R. 2010, *MNRAS*, 405, 436
- Jaffe, W. J., & Perola, G. C. 1973, *A&A*, 26, 423
- Jamrozy, M., Konar, C., Machalski, J., & Saikia, D. J. 2008, *MNRAS*, 385, 1286
- Kaiser, C. R., & Alexander, P. 1997, *MNRAS*, 286, 215
- Kardashev, N. S. 1962, *Soviet Ast.*, 6, 317
- Konar, C., & Hardcastle, M. J. 2013, *MNRAS*, 436, 1595
- Lara, L., Cotton, W. D., Feretti, L., et al. 2001, *A&A*, 370, 409
- Liu, F. K., Wu, X.-B., & Cao, S. L. 2003, *MNRAS*, 340, 411
- Machalski, J., Jamrozy, M., & Zola, S. 2001, *A&A*, 371, 445
- Machalski, J., Jamrozy, M., Zola, S., & Koziel, D. 2006, *A&A*, 454, 85
- Machalski, J., Koziel-Wierzbowska, D., Jamrozy, M., & Saikia, D. J. 2008, *ApJ*, 679, 149-155
- Mack, K.-H., Klein, U., O’Dea, C. P., Willis, A. G., & Saripalli, L. 1998, *A&A*, 329, 431
- Moffet, A. T. 1975, *Galaxies and the Universe*, 211
- Pacholczyk, A. G. 1970, *Series of Books in Astronomy and Astrophysics*, San Francisco: Freeman, 1970,
- Proctor, D. D. 2016, *ApJS*, 224, 18
- Saripalli, L., Hunstead, R. W., Subrahmanyan, R., & Boyce, E. 2005, *AJ*, 130, 896
- Saripalli, L., & Subrahmanyan, R. 2009, *ApJ*, 695, 156
- Schoenmakers, A. P., Mack, K.-H., de Bruyn, A. G., et al. 2000, *A&AS*, 146, 293
- Schoenmakers, A. P., de Bruyn, A. G., Röttgering, H. J. A., & van der Laan, H. 2001, *A&A*, 374, 861
- Solovoyov, D. I., & Verkhodanov, O. V. 2014, *Astrophysical Bulletin*, 69, 141
- Subrahmanyan, R., Saripalli, L., & Hunstead, R. W. 1996, *MNRAS*, 279, 257
- Tamhane, P., Wadadekar, Y., Basu, A., et al. 2015, *MNRAS*, 453, 2438

This paper has been typeset from a $\text{\TeX}/\text{\LaTeX}$ file prepared by the author.